

# Controlled Multifactorial Coagulopathy: Effects of Dilution, Hypothermia, and Acidosis on Thrombin Generation In Vitro

Alexander Y. Mitrophanov, PhD,\*† Fania Szlam, MMSc,‡ Roman M. Sniecinski, MD,‡ Jerrold H. Levy, MD,§ and Jaques Reifman, PhD†

**BACKGROUND:** Coagulopathy and hemostatic abnormalities remain a challenge in patients following trauma and major surgery. Coagulopathy in this setting has a multifactorial nature due to tissue injury, hemodilution, hypothermia, and acidosis, the severity of which may vary. In this study, we combined computational kinetic modeling and in vitro experimentation to investigate the effects of multifactorial coagulopathy on thrombin, the central enzyme in the coagulation system.

**METHODS:** We measured thrombin generation in platelet-poor plasma from 10 healthy volunteers using the calibrated automated thrombogram assay (CAT). We considered 3 temperature levels (31°C, 34°C, and 37°C), 3 pH levels (6.9, 7.1, and 7.4), and 3 degrees of dilution with normal saline (no dilution, 3-fold dilution, and 5-fold dilution). We measured thrombin-generation time courses for all possible combinations of these conditions. For each combination, we analyzed 2 scenarios: without and with (15 nM) supplementation of thrombomodulin, a key natural regulator of thrombin generation. For each measured thrombin time course, we recorded 5 quantitative parameters and analyzed them using multivariable regression. Moreover, for multiple combinations of coagulopathic conditions, we performed routine coagulation tests: prothrombin time (PT) and activated partial thromboplastin time (aPTT). We compared the experimental results with simulations using a newly developed version of our computational kinetic model of blood coagulation.

**RESULTS:** Regression analysis allowed us to identify trends in our data ( $P < 10^{-5}$ ). In both model simulations and experiments, dilution progressively reduced the peak of thrombin generation. However, we did not experimentally detect the model-predicted delay in the onset of thrombin generation. In accord with the model predictions, hypothermia delayed the onset of thrombin generation; it also increased the thrombin peak time (up to 1.30-fold). Moreover, as predicted by the kinetic model, the experiments showed that hypothermia increased the area under the thrombin curve (up to 1.97-fold); it also increased the height of the thrombin peak (up to 1.48-fold). Progressive acidosis reduced the velocity index by up to 24%; acidosis-induced changes in other thrombin generation parameters were much smaller or none. Acidosis increased PT by 14% but did not influence aPTT. In contrast, dilution markedly prolonged both PT and aPTT. In our experiments, thrombomodulin affected thrombin-generation parameters mainly in undiluted plasma.

**CONCLUSIONS:** Dilution with normal saline reduced the amount of generated thrombin, whereas hypothermia increased it and delayed the time of thrombin accumulation. In contrast, acidosis in vitro had little effect on thrombin generation. (Anesth Analg 2020;130:1063–76)

## KEY POINTS

- **Question:** What are the distinct effects of dilution, hypothermia, and acidosis on in vitro thrombin generation in human plasma?
- **Findings:** Dilution reduced the amount of generated thrombin, hypothermia delayed thrombin generation but increased the area under the thrombin curve, and acidosis had practically no effect on thrombin generation.
- **Meaning:** Dilution inhibits thrombin generation, hypothermia contributes to its enhancement, and acidosis induced in vitro does not bring about significant thrombin-generation abnormalities.

## GLOSSARY

**aPTT** = activated partial thromboplastin time; **CAT** = calibrated automated thrombogram; **ETP** = endogenous thrombin potential (ie, the area under the thrombin curve); **FII** = coagulation factor II; **FV** = coagulation factor V; **FVII** = coagulation factor VII; **FVIII** = coagulation factor VIII; **FIX** = coagulation factor IX; **FX** = coagulation factor X; **HCl** = hydrochloric acid; **LT** = lag time; **PPP** = platelet-poor plasma; **PH** = thrombin peak height; **PT** = prothrombin time; **SD** = standard deviation; **TF** = tissue factor; **ttP** = time to thrombin peak; **VI** = velocity index

From the \*The Henry M. Jackson Foundation for the Advancement of Military Medicine, Inc, Bethesda, Maryland; †DoD Biotechnology High Performance Computing Software Applications Institute (BHSAI), Copyright © 2019 International Anesthesia Research Society  
DOI: 10.1213/ANE.0000000000004479

Telemedicine and Advanced Technology Research Center, US Army Medical Research and Development Command, Ft Detrick, Maryland; ‡Department of Anesthesiology, Emory University School of Medicine, Atlanta, Georgia; and §Departments of Anesthesiology, Critical Care, and Surgery, Duke University School of Medicine, Durham, North Carolina.

In civilian and military settings, coagulopathy remains a complex problem in trauma and surgical care.<sup>1,2</sup> Several conditions can contribute to coagulopathy, including hypothermia, metabolic acidosis, and dilution of coagulation proteins and their consumption caused by massive trauma and bleeding.<sup>1-3</sup> While the question of optimal coagulopathy treatments has long been investigated, fully satisfactory answers—in terms of treatment efficacy, safety, and scope of applicability—remain elusive.

The search for advanced therapeutic approaches requires a mechanistic understanding of the effects of coagulopathic conditions on the functional properties of the blood coagulation system. This has been investigated in computational studies<sup>4-10</sup> and laboratory experiments, with coagulopathy induced in vitro<sup>7,11-18</sup> or in vivo (in animal models).<sup>19-26</sup> A major advantage of the purely in vitro strategies is the possibility—at least, in principle—to accurately control the type and intensity of the coagulopathic conditions present. Another advantage is the opportunity to study human whole blood or plasma, with obvious relevance for the investigation of intersubject variability in human abnormal states. Because clinical coagulopathy is likely to be multifactorial,<sup>2</sup> a key element for the design of coagulopathy studies in vitro is the simultaneous presence of several conditions implicated in coagulopathy. However, only few studies to date have been designed in this way.<sup>11,14,27,28</sup> Most such studies have used the viscoelastic properties of blood as the primary end points (in assays such as thromboelastometry).

Here, we investigated the effects of multifactorial coagulopathy on the generation of thrombin, because thrombin is the central enzyme of the blood

coagulation system<sup>29</sup> and impairment of its generation is regarded as the main cause of coagulopathic bleeding.<sup>3</sup> We induced dilution, hypothermia (temperature <37°C), and acidosis (pH < 7.4) in human plasma samples and measured the kinetics of thrombin generation. This in vitro approach allowed us to implement a factorial design to tease out the effects of individual coagulopathic conditions during their simultaneous variation. Furthermore, we compared the experimental results with the outputs of a computational model that we had constructed using available mechanistic information on blood coagulation biochemistry. The use of computational models is becoming increasingly common in coagulation research.<sup>4,8,9,30</sup>

The main objective of our study was to elucidate the effects of the distinct coagulopathic conditions on the quantitative characteristics of the time courses of thrombin generation triggered by tissue factor (TF). TF is the protein that is regarded as the main physiological trigger of thrombin generation.<sup>31</sup> Our hypothesis was that each coagulopathic condition, alone or in combination with other coagulopathic conditions, progressively impaired thrombin generation.

## METHODS

This study was approved by the Human Research Protection Office, Office of Research Protections, US Army Medical Research and Development Command (Ft Detrick, MD), and by the institutional review board of Emory University (Atlanta, GA). The computational-modeling phase of this research was performed at the DoD Biotechnology High Performance Computing Software Applications Institute, whereas the experimental phase was conducted at the Emory University School of Medicine.

## Subject Group

Subjects were recruited at the Emory University School of Medicine. All subjects (healthy volunteers) gave written informed consent to participate in this study. The subject group consisted of 10 individuals (5 women and 5 men, between ages 21 and 65) who had no preexisting blood-clotting abnormalities and were not taking any medications known to affect coagulation testing.

## Blood Sample Collection and Plasma Preparation

Blood samples (50 mL) were drawn from each volunteer. Most of the blood (48 mL) was placed into 3.2% citrate Vacutainer tubes (Becton-Dickinson, Franklin Lakes, NJ) to be used for coagulation and thrombin-generation studies. The remaining blood (2 mL) was collected into a K2-EDTA tube for hematology testing. Counts of white blood cells, hematocrit, hemoglobin, platelets, and other hematological parameters were determined using a pocH-100i

Accepted for publication September 10, 2019.

Funding: This research was supported by the US Army Network Science Initiative, US Army Medical Research and Development Command, Ft Detrick, MD.

The authors declare no conflicts of interest.

Supplemental digital content is available for this article. Direct URL citations appear in the printed text and are provided in the HTML and PDF versions of this article on the journal's website ([www.anesthesia-analgesia.org](http://www.anesthesia-analgesia.org)).

The computer code implementing our kinetic model is available from the authors on request.

The opinions and assertions contained herein are private views of the authors and are not to be construed as official or as reflecting the views of the US Army, the US Department of Defense, or The Henry M. Jackson Foundation for the Advancement of Military Medicine, Inc. This paper has been approved for public release with unlimited distribution.

Reprints will not be available from the authors.

Address correspondence to Alexander Y. Mitrophanov, PhD, DoD Biotechnology High Performance Computing Software Applications Institute, Telemedicine and Advanced Technology Research Center, US Army Medical Research and Development Command, ATTN: FCMR-TT, 504 Scott St, Ft Detrick, MD 21702. Address e-mail to [alex@bhsai.org](mailto:alex@bhsai.org); and Jaques Reifman, PhD, DoD Biotechnology High Performance Computing Software Applications Institute, Telemedicine and Advanced Technology Research Center, US Army Medical Research and Development Command, ATTN: FCMR-TT, 504 Scott St, Ft Detrick, MD 21702. Address e-mail to [jaques.reifman.civ@mail.mil](mailto:jaques.reifman.civ@mail.mil).

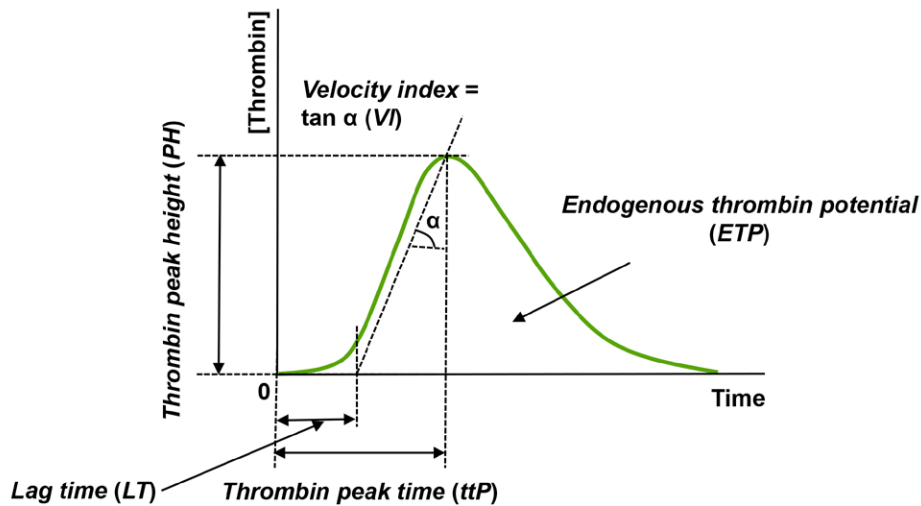
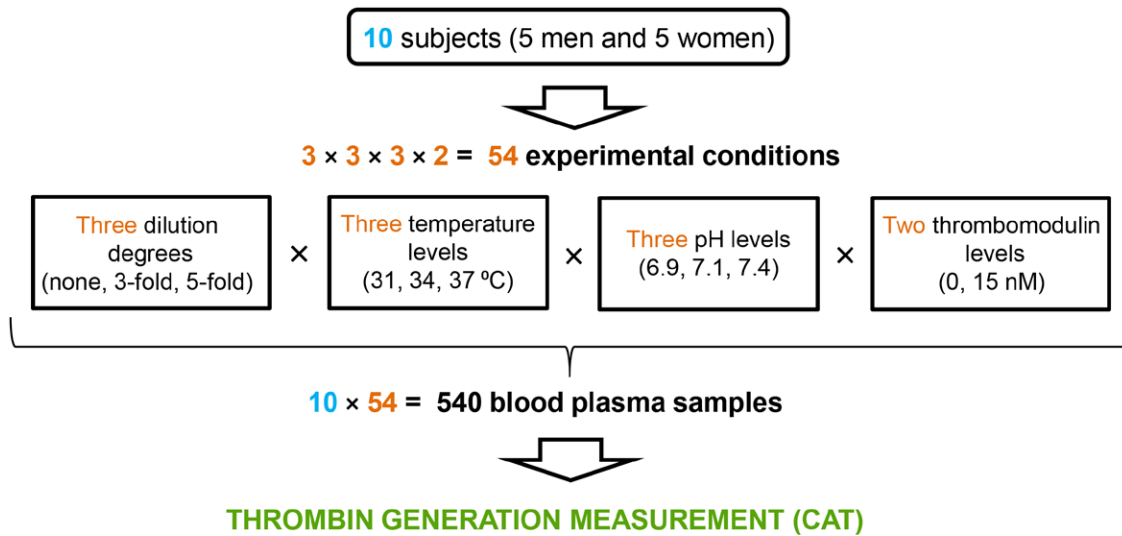


**Figure 1.** Experimental design for the study. For each subject ( $n = 10$ ), collected blood samples were used to prepare PPP. PPP samples were used to generate an array of experimental conditions mimicking multifactorial coagulopathy. A temperature level of 37°C, pH 7.4, and no plasma dilution were regarded as normal physiological conditions, and deviations from these levels represented coagulopathic states. Thrombin-generation time courses were measured using the CAT assay, and the following 5 quantitative parameters (see definitions in the Methods section) were evaluated: LT, ttP, VI, PH, and ETP. The parameters LT, ttP and VI are often regarded as the “timing” parameters, whereas PH and ETP are the “amount” parameters because the first and the second parameter groups characterize the rate of thrombin generation and the amount of generated thrombin, respectively. CAT indicates calibrated automated thrombogram; ETP, endogenous thrombin potential; LT, lag time; PH, thrombin peak height; PPP, platelet-poor plasma; ttP, time to thrombin peak; VI, velocity index.

series Coulter Analyzer (Sysmex Corp, Lincolnshire, IL) to verify the absence of any gross hematological abnormality.

Our experiments were conducted in platelet-poor plasma (PPP). The use of PPP is a frequent approach to thrombin-generation measurement in plasma, leveraging thoroughly tested experimental protocols for reliable acquisition of data directly comparable with published research.<sup>7,32–35</sup> Citrated blood samples were centrifuged for 20 minutes at 2000g at room temperature in a refrigerated centrifuge fitted with a swinging bucket rotor. The PPP layer was carefully removed, checked for residual platelets, aliquoted into 1-mL storage tubes, and stored at –80°C until the time of analysis.

**Induction of Dilution, Hypothermia, and Acidosis**

At the time of analysis, frozen plasma aliquots were thawed in a 37°C water bath for ~3–5 minutes and then immediately used in the experiments. Figure 1 shows the design of our experimental study. Briefly, the PPP samples were diluted, acidified, or temperature-adjusted to induce conditions mimicking multifactorial coagulopathy. In those samples, we performed routine coagulation tests (prothrombin time [PT] and activated partial thromboplastin time [aPTT]) and a thrombin-generation assay, which measures thrombin time courses.

To prepare diluted samples, thawed plasma samples were diluted (by volume, v/v) 3- or 5-fold with normal saline (0.9% NaCl) (corresponding to 33.3%

and 20% of the remaining plasma, respectively). Our choice of normal saline as diluent was based on its extensive history of use as both a resuscitation fluid<sup>36</sup> and a priming solution in cardiac surgery.<sup>37</sup> The fidelity of our plasma-dilution protocol was verified in a recent study.<sup>7</sup> For the experiments involving pH adjustments, dilute hydrochloric acid (HCl) of increased normality (0.25, 0.5, 1.0, and 2.0 N) was used to achieve a plasma pH of 7.4, 7.1, or 6.9 (the pH of thawed plasma can slightly differ from 7.4). The FluCa reagent (Fluo-Buffer with Fluo-Substrate; Diagnostica Stago, Parsippany, NJ) and the TF activator (Diagnostica Stago, Parsippany, NJ) needed for thrombin-generation measurement (see below) were also pH-adjusted accordingly. Dilute sodium hydroxide solution (0.25–1 N) was also used in the pH adjustments as needed. All pH adjustments were performed using an Orion Star A211 Benchtop Meter fitted with a ROSS Ultra Triode glass-body pH/ATC electrode (ThermoScientific Orion, Beverly, MA). Thrombin generation (see below) was measured at a preset temperature of 37°C, 34°C, or 31°C.

In some experiments, thrombomodulin (Sigma Aldrich, St Louis, MO; final concentration, 15 nM) was added to the diluted and undiluted plasma samples to evaluate its effects on thrombin generation and on the PT and aPTT measurements. Thrombomodulin is a protein that strongly enhances thrombin-dependent activation of protein C, which is one of the main negative regulators of thrombin generation in plasma.<sup>38</sup> Because in the vasculature thrombomodulin is predominantly expressed on the surfaces of endothelial cells, it has to be added externally for *in vitro* assays. By adding thrombomodulin, we aimed to explore the effects of the protein C mechanism on thrombin generation under coagulopathic conditions.

PT and aPTT were measured at 37°C only, using the STA Compact Analyzer (Diagnostica Stago, Parsippany, NJ). The PT reagent contained Ca<sup>2+</sup> thromboplastin, which is a mixture of Ca<sup>2+</sup>, TF, and a specific heparin inhibitor. The aPTT reagent contained rabbit cephalin and silica as an activator. pH adjustment and thrombomodulin supplementation resulted in <1% additional sample dilution and therefore did not affect the results of subsequent analyses.

### Thrombin-Generation Measurement

Thrombin generation was measured using the Calibrated Automated Thrombogram (CAT) assay (Diagnostica Stago, Parsippany, NJ) described by Hemker et al.<sup>33</sup> The final TF concentration in the samples was 5 pM. This is one of the standard TF concentrations for thrombin-generation measurement,<sup>4,33,34,39</sup> and this choice was consistent with our previous research.<sup>5–7,32</sup> Moreover, this TF concentration yields *in vitro* clotting times that are comparable

with *in vivo* bleeding times.<sup>31,39</sup> Thrombin generation was measured using equipment and reagents from Diagnostica Stago, and progress of the thrombin-generation reaction was continually monitored for 60–90 minutes. The reagents for thrombin generation contained phospholipids, which supported thrombin generation in the absence of platelets.

Briefly, for each experiment, the microtiter plate containing the PPP samples was incubated for 10 minutes at a preset temperature and pH in the CAT instrument, and then the thrombin-generation reaction was started automatically by the addition of 20 µL/well of the temperature- and pH-adjusted FluCa reagent. All samples were run in duplicate. The Thrombinoscope software (Diagnostica Stago, Parsippany, NJ) was used to record the experimental readouts and to calculate the thrombin-generation parameters. We recorded the following quantitative parameters of thrombin generation:<sup>7</sup> lag time (LT, time to 1/6 of the thrombin peak), thrombin peak time (or time to thrombin peak [ttP]), thrombin peak height (PH), the velocity index (VI, calculated as PH/[ttP – LT], approximating the slope of the thrombin time course), and endogenous thrombin potential (ETP, the area under the thrombin curve; Figure 1). LT and VI characterize the earliest phase of thrombin generation (before thrombin peak is reached); the remaining 3 parameters reflect later thrombin-generation phases—propagation and termination.<sup>30,40</sup>

### Blood Coagulation Protein Measurement in PPP

To parameterize our kinetic model (see the next subsection and Supplemental Digital Content, Document, <http://links.lww.com/AA/C947>), we measured the plasma levels of the main coagulation proteins (specifically, coagulation factors [F] II, FV, FVII, FVIII, FIX, FX, antithrombin, TF pathway inhibitor, protein C, and fibrinogen). The details regarding the measurements are given in Supplemental Digital Content, Document, <http://links.lww.com/AA/C947>.

### Computational Kinetic Modeling

The computational kinetic model of blood coagulation biochemistry used in this study is an extension of our previously developed integrated model of thrombin generation, fibrin formation, and fibrinolysis.<sup>41</sup> The model framework reflects the current biochemical knowledge about the blood coagulation system, which is based on *in vitro* experiments. Whereas our focus in this study is on thrombin generation, the inclusion of the fibrin formation and fibrinolysis reactions makes our model more complete and potentially applicable to a wider range of experimental conditions. The model did not take into account platelet activity, because it reflected thrombin generation primarily in systems where catalytic surfaces are

provided by externally supplemented phospholipids, such as our experimental assay.<sup>7,30,41</sup>

The model is a system of 107 differential equations, in which each equation relates the rate of change in the concentration of a biochemical species with the concentrations of other species according to the standard chemical-kinetics modeling methodology<sup>42</sup> (most of the kinetics in the model are mass-action). Numerical solution of these equations on the computer produces the model outputs, which are the time courses for the concentrations of each of the 107 represented biochemical species. The main model output analyzed in this study was the thrombin time course. Besides the reactions for thrombin generation, fibrin formation, and fibrinolysis, the model used here contains several reactions (taken from Mitrophanov et al<sup>7</sup>) that are specific to the CAT assay and can affect the thrombin readout. Supplemental Digital Content, Table S1, <http://links.lww.com/AA/C947>, shows the full list of the biochemical reactions constituting the model (here and elsewhere, the designation “S” for figures and tables indicates Supplemental Digital Content, Document, <http://links.lww.com/AA/C947>). In addition to the reactions on the list, the model was defined by the numerical values of the 120 reaction rate and equilibrium constants (their default values also are given in Supplemental Digital Content, Table S1, <http://links.lww.com/AA/C947>) and the initial concentrations of the biochemical species (ie, their concentrations at time 0, when thrombin generation starts; the default values are given in Supplemental Digital Content, Table S2, <http://links.lww.com/AA/C947>). These initial concentrations constitute the main model inputs; they can be obtained from coagulation protein measurements in plasma samples for individual subjects, which allowed us to perform subject-specific simulations. In the software we used to define the model and run the simulations (MATLAB R2017b; MathWorks, Inc, Natick, MA), the reaction list and parameter values from Supplemental Digital Content, Tables S1 and S2, <http://links.lww.com/AA/C947>, were used directly to specify the model (via the graphical user interface of the SimBiology toolbox), and the mathematical equations constituting the model were generated by MATLAB automatically. The initial concentrations and kinetic parameters in the model were modulated to reflect dilution,<sup>7,41,43</sup> hypothermia,<sup>5</sup> and acidosis<sup>6</sup> following our previous study. Supplemental Digital Content, Document, <http://links.lww.com/AA/C947>, provides further details on the computational modeling.

### Statistical Analysis

Our initial sample size determination was based on the *in vitro* coagulopathy (hypothermia + acidosis) study by Dirkmann et al,<sup>11</sup> where we used, for

example, clotting time values (mean  $\pm$  1 standard deviation [SD]) of  $65 \pm 11.86$  seconds as end points for our determination (from Figure 2A of that article). We used values reported in the study and the MATLAB function “*sampsizepwr*” to determine a sample size sufficient to detect 2-fold changes in statistical sample comparisons at a significance level of .05 and power level of 0.8. We then performed a similar analysis using lag time values measured using CAT:  $1.6 \pm 0.4$  minutes (Figure 5B from Mitrophanov et al<sup>7</sup>). These analyses indicated sufficiency of the sample size (ie, the number of subjects)  $n = 10$ . For our regression analysis (see below), this translated into  $10$  (subjects)  $\times$   $54$  (experimental conditions in the factorial design) =  $540$  unique data points per each output variable.

We analyzed our experimental measurements using stepwise multivariable regression. In this analysis, we had 4 independent variables: degree of dilution, temperature, pH, and thrombomodulin concentration. These variables were scaled to vary in the range  $(-1, 1)$  (min-max scaling). For each of the 5 thrombin-generation parameters, we first wrote the full regression equation, which contained single-variable terms and 2-, 3-, and 4-way interaction terms. For PT and aPTT, we wrote similar full equations, but they did not contain the temperature dependence (because PT and aPTT measurements were performed at a constant temperature). Besides the linear single-variable terms, the full regression equations contained a quadratic term for the degree of dilution. We introduced this term to capture the pronounced nonmonotonic dependencies of VI, PH, and the ETP on the degree of dilution in the case of 15 nM supplemented thrombomodulin (see the Results section). Moreover, adding this quadratic term considerably improved the regression results for PT and aPTT (ie, made the residual scatter plot more symmetrical around the line  $x = 0$ ).

We then used the stepwise regression routine (MATLAB function “*stepwiselm*”) to reduce the equations, keeping only the most relevant terms. The *P* value tolerances for removing or adding regression-equation terms were set to .050 and .049, respectively (the “*stepwiselm*” function required that the latter tolerance be less than the former one). We then compared the coefficients of these reduced regression equations with the outputs of the MATLAB function “*fitrm*,” which we also used to fit the initial (ie, full) regression equations to our data. This function had been developed specifically for repeated-measures regression, but it does not perform stepwise elimination of regression terms. The coefficients in the reduced regression equations were numerically close to the corresponding coefficient values in the full regression equations fitted using “*fitrm*,” indicating that “*stepwiselm*”

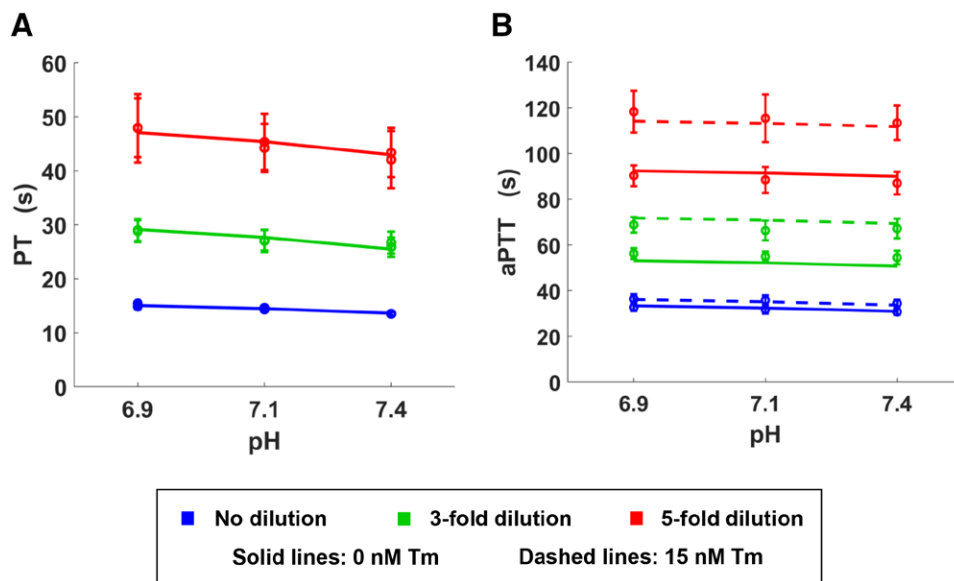


**Figure 2.** Standard coagulation tests under different experimental conditions (at a temperature of 37°C). A, PT. B, aPTT. The experimental points (circles) and error bars represent mean  $\pm$  1 SD ( $n = 10$ ). Blue, green, and red lines show the outputs of our regression models and indicate no dilution, 3-fold dilution, and 5-fold dilution, respectively. Solid and dashed lines correspond to 0 and 15 nM supplemented Tm (in the figure), respectively. For PT, the solid and dashed lines overlap. aPTT indicates activated partial thromboplastin time; PT, prothrombin time; SD, standard deviation; Tm, thrombomodulin.

captured the effects of the main predictors and indeed eliminated the terms of small influence.

In the resultant reduced equations, we compared the relative magnitudes of the regression coefficients to identify the most influential coagulopathic conditions and to interpret the trends in our data. See Supplemental Digital Content, Document, the Regression Analysis Section, <http://links.lww.com/AA/C947>, for further methodological details and regression-equation definitions. The reported fold changes for the experimental data were obtained from the fitted regression values, and the fold changes for the kinetic model simulations were calculated as ratios of the sample means.

## RESULTS

### PT, aPTT, and Coagulation Protein Measurements

The standard hematological indices were in the normal ranges for each of the 10 subjects (see Supplemental Digital Content, Document, <http://links.lww.com/AA/C947>). Coagulation protein levels for all 10 subjects are shown in Supplemental Digital Content, Table S3, <http://links.lww.com/AA/C947>. The corresponding mean concentrations ( $\pm$ 1 SD) were as follows: FII ( $100.6 \pm 15.6\%$ ), FV ( $104.5 \pm 12.7\%$ ), FVII ( $110.5 \pm 23.1\%$ ), FVIII ( $133.1 \pm 40.5\%$ ), FIX ( $125.2 \pm 31.8\%$ ), FX ( $110.7 \pm 20.5\%$ ), antithrombin ( $105.0 \pm 10.1\%$ ), protein C ( $119.5 \pm 25.6\%$ ), TF pathway inhibitor ( $8.2 \pm 2.0$  ng/mL), and fibrinogen ( $277.2 \pm 39.8$  mg/mL).

Multivariable regression analysis yielded regression equations for PT and aPTT ( $P < 10^{-5}$ ). Based on this analysis, both PT and aPTT progressively increased with plasma dilution, in accord with the PT simulations performed in our earlier study.<sup>5</sup>

Acidosis increased PT only slightly (up to  $\sim$ 1.14-fold; Figure 2A), and it affected aPTT even less (Figure 2B).

### Time Courses of Thrombin Generation

We computationally simulated and experimentally measured thrombin time courses for each of the 10 subjects and under each condition shown in Figure 1. The time courses had the expected, typical one-peaked shape (Figures 3–4). Visual inspection of the time courses immediately highlighted prominent patterns characterizing the dependency of thrombin generation on dilution and pH. Figure 3 shows both our simulation results and experimental data on thrombin generation for physiological pH (ie, 7.4) and the default condition of zero externally added thrombomodulin. The computational kinetic model captured the main trends in the data at a semiquantitative level. We emphasize that because the data reported here were not used to develop our kinetic model, all simulation–experiment comparisons constitute “pure validation.”

For both the computations and experiments, thrombin levels near the time-course peak (but not necessarily at the tail) progressively decreased as the degree of dilution increased (Figure 3). The computational kinetic model predicted a progressive, dilution-dependent delay in the onset of thrombin generation (ie, the time when the thrombin level begins to visibly increase) and in the appearance of the thrombin peak (Figure 3A–C). In contrast, the experimental data demonstrated insensitivity of the time of thrombin-generation onset and of the peak time to dilution (Figure 3D–F). We anticipated these outcomes because they agree with our earlier simulation results<sup>7,43</sup> and

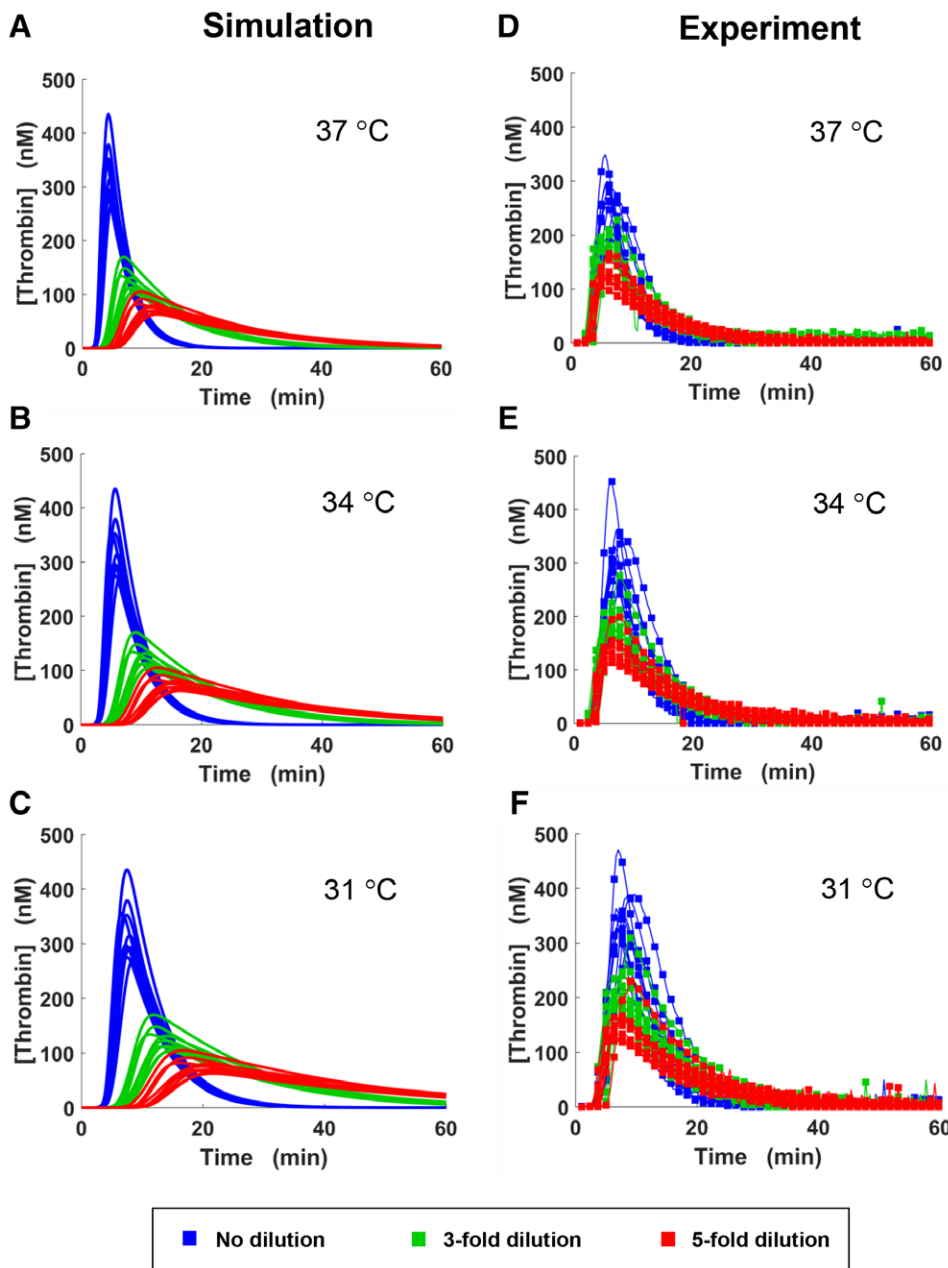


**Figure 3.** Thrombin-generation time courses for each subject ( $n = 10$ ) at pH 7.4 without supplemented thrombomodulin. A–C, Computational model simulations. D–F, Experimental results obtained using the CAT assay. Blue, green, and red lines indicate no dilution, 3-fold dilution, and 5-fold dilution, respectively. A and D, 37°C. B and E, 34°C. C and F, 31°C. CAT indicates calibrated automated thrombogram.

thrombin-generation experiments using a similar *in vitro* setup.<sup>7,32,44</sup> Although our simulations overestimated the dilution-induced delay in thrombin-generation onset, we previously predicted that PH is considerably more sensitive to dilution than is clotting time (a parameter analogous to LT characterizing the onset of thrombin generation).<sup>43</sup> Our experimental results are fully consistent with this prediction (Figure 3D–F).

The overall influence of acidosis on thrombin generation can be assessed by comparing the results shown in Figure 3 with analogous results for pH 6.9 (Figure 4; the data for the intermediate pH level of 7.1 follow the same trend and are shown in

Supplemental Digital Content, Figure S1, <http://links.lww.com/AA/C947>). Our kinetic model predicted a considerable delay and overall reduction in thrombin generation under acidotic conditions (Figure 4A–C). Expectedly, these results are consistent with our earlier computational simulations of the impact of pH changes on thrombin generation.<sup>6</sup> The pH-dependent reduction in the height of the model-simulated thrombin peak was particularly pronounced under the no-dilution conditions (Figure 4A–C, blue lines). In contrast, rather surprisingly, our experimental data did not display large systematic differences on pH level variation (Figure 4D–F).

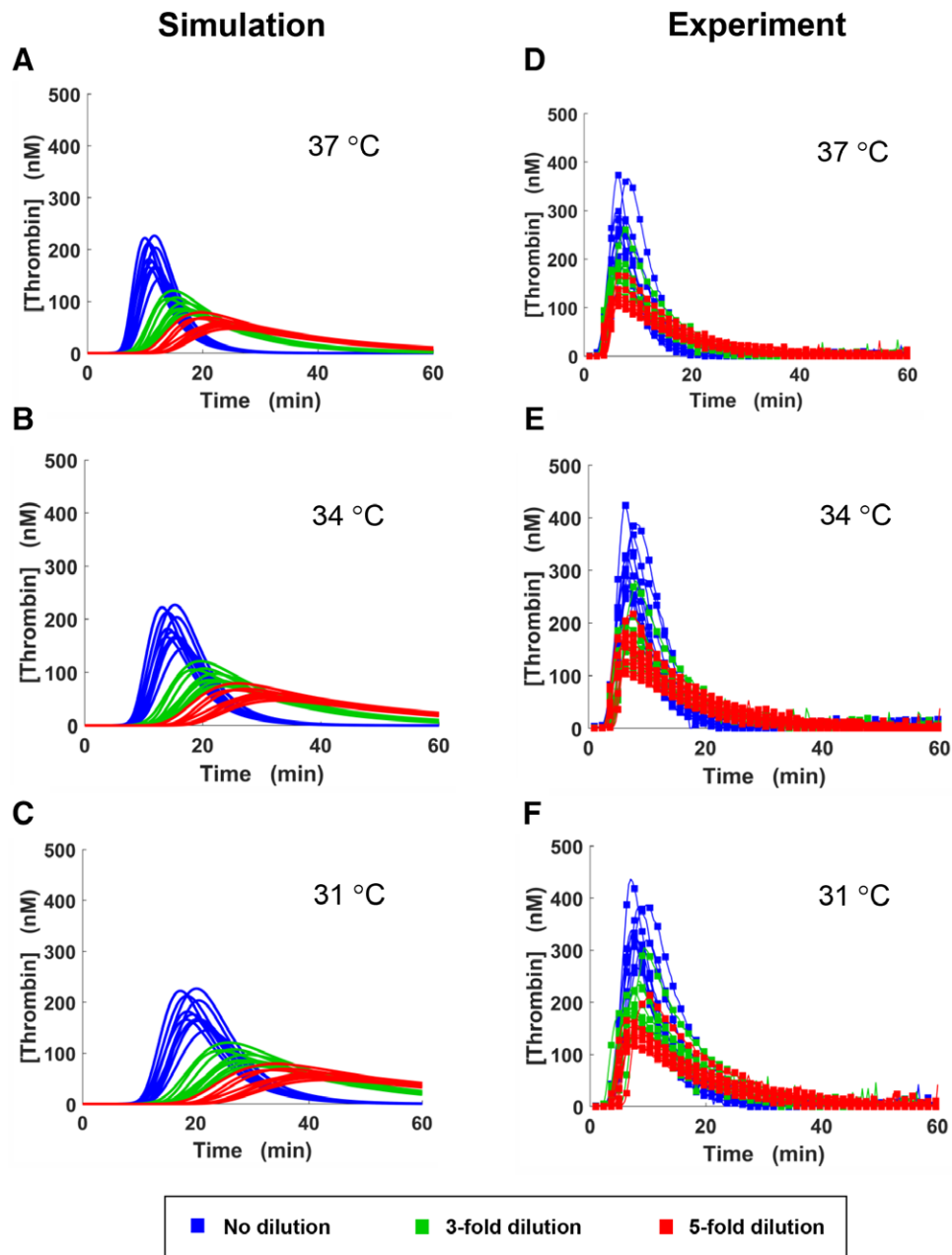


**Figure 4.** Thrombin-generation time courses for each subject ( $n = 10$ ) at pH 6.9 without supplemented thrombomodulin. A–C, Computational model simulations. D–F, Experimental results obtained using the CAT assay. Blue, green, and red lines indicate no dilution, 3-fold dilution, and 5-fold dilution, respectively. A and D, 37°C. B and E, 34°C; C and F, 31°C. CAT indicates calibrated automated thrombogram.

### Quantitative Parameters of Thrombin Generation

Our multivariable regression analysis yielded regression equations ( $P < 10^{-5}$ ) for each of the thrombin-generation parameters defined in Figure 1. As an illustration, Figure 5 shows the experimental results and the regression outputs for LT (which approximates the time of thrombin-generation onset; Figure 5A–C), and VI (which approximates the left-hand slope of the thrombin peak; Figure 5D–F). Supplemental Digital Content, Figure S2, <http://links.lww.com/AA/C947>, shows the corresponding kinetic model simulation results. In accordance with our analysis of

the thrombin time courses (Figures 3–4), the simulation results considerably overpredicted the effects of dilution and acidosis on lag time. The simulations predicted that hypothermia should increase the lag time (Figure 3A–C), which would be particularly pronounced for low pH (Figure 4A–C). Consistent with the prediction, the lag time increased for low temperature values (Figure 5A–C). According to the regression analysis, dilution had a weaker (than temperature) effect on lag time, and pH had the weakest effect on lag time. The effects of thrombomodulin on lag time were small, particularly so in diluted plasma

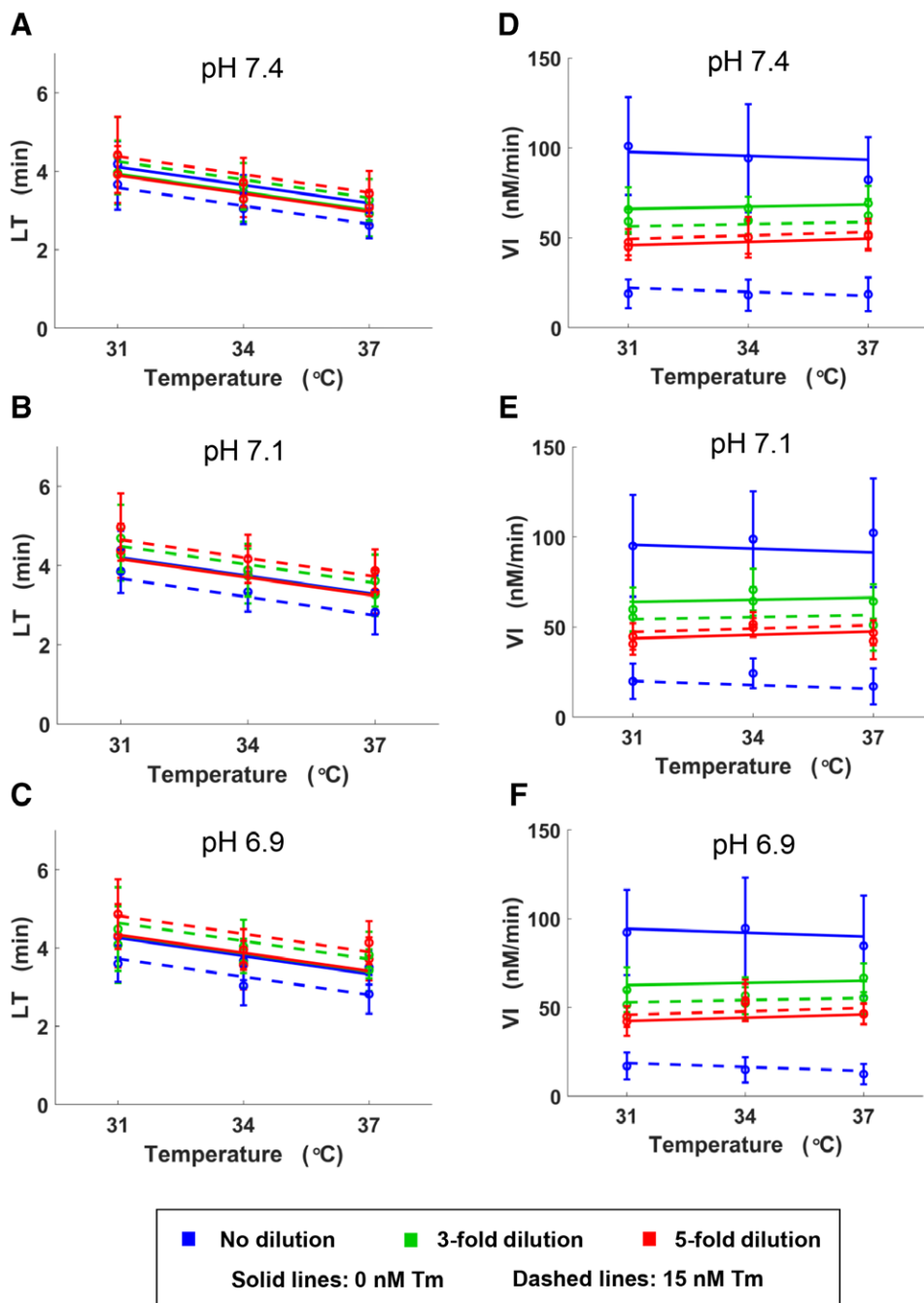


**Figure 5.** Quantitative parameters of thrombin generation under different experimental conditions. The parameter values were derived from thrombin time courses measured using the CAT assay. A–C, LT. D–F, VI. The experimental points (circles) and error bars represent mean  $\pm$  1 SD ( $n = 10$ ). Blue, green, and red lines show the outputs of our regression models and indicate no dilution, 3-fold dilution, and 5-fold dilution, respectively. Solid and dashed lines correspond to 0 and 15 nM supplemented Tm, respectively. A and D, pH 7.4. B and E, pH 7.1. C and F, pH 6.9. CAT indicates calibrated automated thrombogram; LT, lag time; SD, standard deviation; Tm, thrombomodulin; VI, velocity index.

(Figure 5A–C). Interestingly, in diluted plasma, thrombomodulin supplementation (which activates protein C, a thrombin-inhibition mechanism) has shortened the lag time. In contrast, in our kinetic simulations, thrombomodulin supplementation resulted in a systematic (albeit minimal in some cases) increase in lag time, consistent with the inhibitory role of protein C (Supplemental Digital Content, Figure S2, A–C, <http://links.lww.com/AA/C947>).

There were considerable discrepancies between the VI values predicted by our model (Supplemental Digital Content, Figure S2, D–F, <http://links.lww.com/AA/C947>) and those derived from experimental data (Figure 2D–F). In the simulations, VI was strongly inhibited by hypothermia and acidosis (consistent with our previous modeling results<sup>5,6</sup>), which can be understood based on the mathematical definition of VI (please see the subsection “Thrombin-Generation Measurement” and Figure 1). Indeed, acidosis strongly inhibited the model-simulated PH (Figures 3A–C, 4A–C), which is proportional to VI. In the case of hypothermia, PH was not affected, but the time of onset of thrombin generation and thrombin peak time were considerably increased

(Figure 5A–C). Interestingly, in diluted plasma, thrombomodulin supplementation (which activates protein C, a thrombin-inhibition mechanism) has shortened the lag time. In contrast, in our kinetic simulations, thrombomodulin supplementation resulted in a systematic (albeit minimal in some cases) increase in lag time, consistent with the inhibitory role of protein C (Supplemental Digital Content, Figure S2, A–C, <http://links.lww.com/AA/C947>) and those derived from experimental data (Figure 2D–F). In the simulations, VI was strongly inhibited by hypothermia and acidosis (consistent with our previous modeling results<sup>5,6</sup>), which can be understood based on the mathematical definition of VI (please see the subsection “Thrombin-Generation Measurement” and Figure 1). Indeed, acidosis strongly inhibited the model-simulated PH (Figures 3A–C, 4A–C), which is proportional to VI. In the case of hypothermia, PH was not affected, but the time of onset of thrombin generation and thrombin peak time were considerably increased

(Figures 3A–C, 4A–C), reducing VI. In contrast, the experimentally determined VI was insensitive to temperature and pH variations due to a weaker dependence of PH, as well as of thrombin onset time and peak time, on these conditions (Figures 3D–F, 4D–F). A distinguishing feature of the VI was its large variation between subjects (coefficient of variation up to 59.11%; Figure 5D–F). This is consistent with our previous computational work, which suggested that the slope of the tangent line for the left-hand side of the thrombin curve (approximated by the VI) tends to be highly sensitive and variable under different conditions.<sup>5,6,43</sup> It is conceivable that the large variability could mask the dependency of the VI on temperature in Figure 5D–F. According to our regression analysis, VI was strongly dominated by dilution.

The regression analysis demonstrated little or no effect of pH on the thrombin-generation parameters in our experimental system. For example, in the final regression equation for lag time, the only pH-dependent term was the smallest in magnitude and at the margin of significance ( $P \approx .05$ ); this resulted in up to only ~1.15-fold acidosis-induced increase in lag time. Acidosis induced changes in thrombin peak time (up to ~1.1-fold increase) and VI (up to ~1.24-fold decrease); acidosis had practically no systematic influence on the magnitude of dilution- or hypothermia-induced effects. The reduced regression equations for peak height and ETP did not contain any pH-dependent terms. For this reason, we focused our further analyses on the combined effects of dilution and temperature. The remaining 3 thrombin parameters—thrombin peak time, PH, and ETP—characterize the later stages of thrombin generation. Figure 6 shows their computationally predicted and experimentally measured values at pH 7.4 (the patterns at pH 6.9 and 7.1 were similar, Supplemental Digital Content, Figure S3, <http://links.lww.com/AA/C947>). Our kinetic model simulations predicted that hypothermia tends to increase thrombin peak time (Figure 6A). This was consistent with our regression analysis; indeed, temperature was the most dominant variable in the regression equation for the peak time. However, the magnitude of the increase was smaller in the experiment (up to a 1.73-fold increase predicted by the kinetic model versus up to a 1.30-fold increase in the experiment). In the experiments and simulations, the effects of thrombomodulin on peak time (Figure 6A, D; Supplemental Digital Content, Figure S3, A, D, <http://links.lww.com/AA/C947>) were similar to those predicted and observed for lag time.

Figure 6B, C, E, F shows computational and experimental results for PH and ETP at pH 7.4 (the pattern was similar at other pH values). The regression analysis identified a progressive hypothermia-induced

increase in both the PH and the ETP, signified by relatively large (in absolute value) negative single-variable regression coefficients for temperature. The kinetic model predicted no significant effect of hypothermia on the PH, which increased up to 1.48-fold in the experiment (this fold change was attained for 15 nM supplemented thrombomodulin; the fold changes were smaller in the experiments without thrombomodulin supplementation). The seemingly counterintuitive ETP increase caused by hypothermia, predicted by our computations (Figure 6C), was consistent with our experimental results (up to a 1.73-fold increase predicted by the model versus up to a 1.97-fold increase in the experiment).

Dilution had a progressive inhibitory effect on the VI (Figure 5D–F), PH (Figure 6E; Supplemental Digital Content, Figure S3, <http://links.lww.com/AA/C947>), and the ETP (Figure 6F; Supplemental Digital Content, Figure S3, <http://links.lww.com/AA/C947>) at 0 nM supplemented thrombomodulin. The sensitivity of VI to dilution was captured by our kinetic model; indeed, the velocity index values for undiluted plasma considerably exceeded those for diluted plasma (Supplemental Digital Content, Figure S2, D–F, <http://links.lww.com/AA/C947>). While the computational model may have underpredicted the effect of dilution on the ETP (Figure 6C, solid lines), the experimentally determined ETP values for different dilution degrees were quite close to each other; in fact, the corresponding error bars strongly overlapped (Figure 6F, solid lines). Thus, the computational model correctly predicted the relative insensitivity of the ETP to dilution. In the experiments, at 15 nM thrombomodulin, the dependency of VI, PH, and the ETP on dilution became non-monotonic, with the smallest values corresponding to undiluted plasma (Figures 5D–F, 6E, F; Supplemental Digital Content, Figure S3, B–C and E–F, <http://links.lww.com/AA/C947>). In the simulations, however, these dependencies followed monotonic patterns consistent with the inhibitory role of thrombomodulin (Figure 6B, C; Supplemental Digital Content, Figure S2, A–C, <http://links.lww.com/AA/C947>). It is conceivable that the discrepancies between the simulations and experiments for 15 nM thrombomodulin were (at least partially) due to a lack of thrombomodulin supplementation in the data set that we had used to calibrate the kinetic model.<sup>7</sup> Indeed, quantitative parameters of in vitro blood coagulation time courses can strongly depend on the details of the experimental setup and protocols,<sup>41</sup> suggesting that the thrombomodulin/protein-C module of our kinetic model needs assay-specific calibration for improved predictive results.

## DISCUSSION

We used predictive computational modeling and in vitro experimentation to investigate the effects

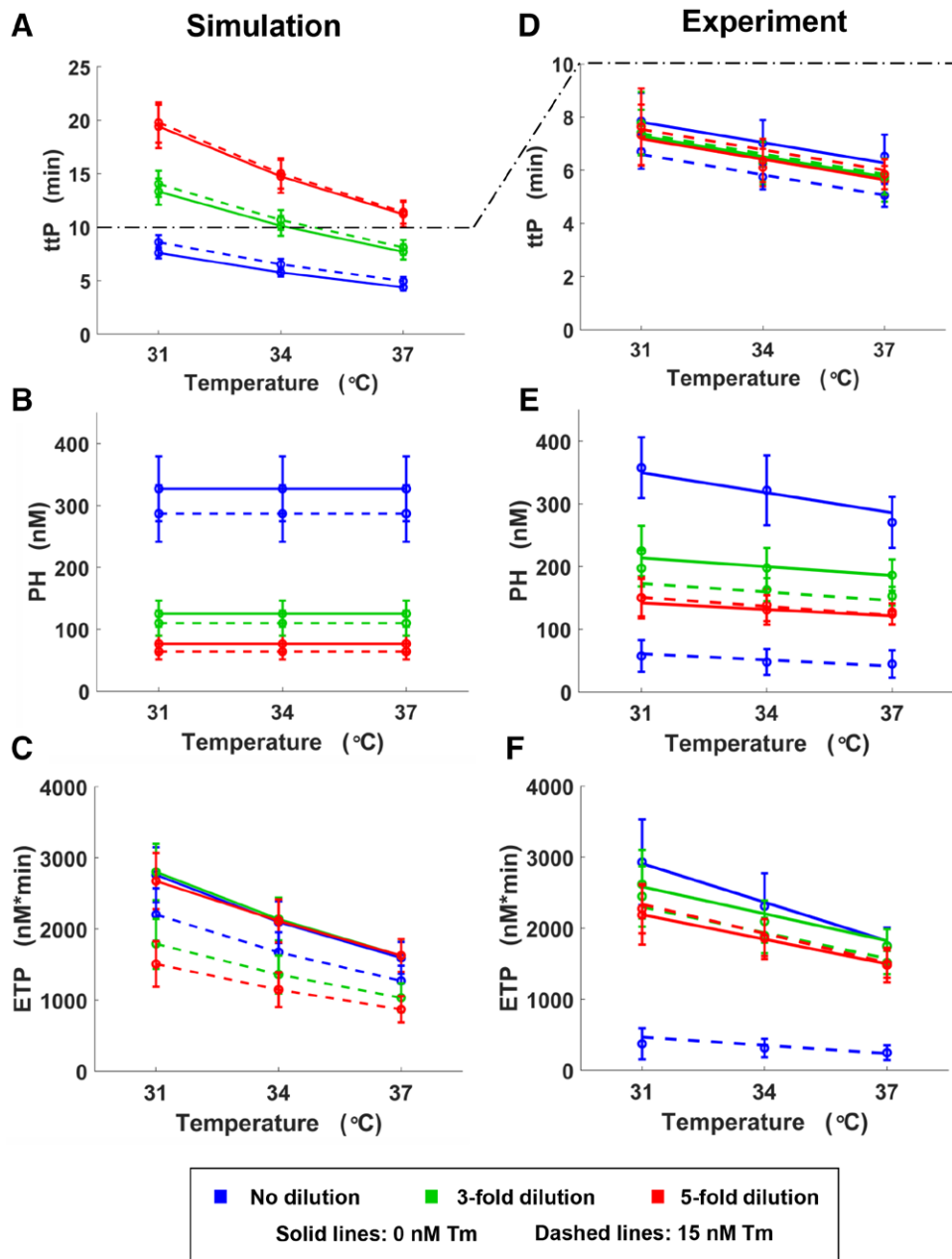


**Figure 6.** Quantitative parameters of thrombin generation under different experimental conditions at pH 7.4. The subplots on the left show computationally simulated results, and those on the right show the corresponding experimental data. A and D, ttP; B and E, PH. C and F, ETP. A and B, The dash-dotted black line shows the mapping between the respective y-axis scales. The experimental points (circles) and error bars represent mean  $\pm$  1 SD ( $n = 10$ ). Blue, green, and red lines indicate no dilution, 3-fold dilution, and 5-fold dilution, respectively. For the subplots on the left, the lines connect the means and are shown to emphasize trends in the data. For the subplots on the right, the lines show the outputs of our regression models. Solid and dashed lines correspond to 0 and 15 nM supplemented Tm, respectively. ETP indicates endogenous thrombin potential; LT, lag time; PH, thrombin peak height; SD, standard deviation; Tm, thrombomodulin; ttP, time to thrombin peak.

of 3 coagulopathic conditions—dilution, hypothermia, and acidosis—on the generation of thrombin in human plasma. The computations predicted several of the experimentally detected dependencies measured using CAT. The CAT assay belongs to the family of “global” assays of hemostasis, whose purpose is to go beyond the assessments provided by the classic diagnostic clinical assays, such as the PT and

aPTT,<sup>45</sup> which terminate when only ~5% of thrombin is generated.<sup>46</sup> While primarily considered a research tool, CAT is emerging as a tool that could provide clinically relevant insights into both hemostasis and thrombosis.<sup>40,45</sup> Indeed, clinical blood coagulation analyses are typically performed using in vitro assays without blood flow; the purpose of CAT is to give a more comprehensive picture of thrombin generation

under such conditions. Thus, *in vitro* analysis can be an informative first step toward a fuller understanding of clinical coagulopathy.

It is conceivable that CAT outputs, such as thrombin-generation parameter values (Figure 1), may contribute to diagnostic and prognostic analyses of blood samples collected from patients.<sup>35,40</sup> Moreover, the usefulness of thrombin-generation parameters stems from their ability to characterize the 3 functional phases of thrombin generation: initiation, propagation, and termination.<sup>30,40</sup> Because *in vivo* blood coagulation strongly relies on thrombin-generation biochemistry,<sup>3</sup> these functional phases could constitute a conceptual framework for the interpretation of clinical data. Yet, certain global assays and the presence of platelets can result in patterns different from those using CAT. Indeed, the results of Dirkmann et al<sup>11</sup> obtained using thromboelastometry in whole blood are consistent with our findings in that acidosis alone did not cause significant changes in coagulation. However, in contrast to our findings, the authors detected a considerable synergistic effect: acidosis exacerbated the impact of hypothermia on clot formation.

The progressive reduction in PH on dilution, detected in our simulations and experiments, is consistent with reported outcomes of *in vivo* blood dilution and with the general notion that dilution and coagulation protein depletion reduce thrombin generation,<sup>21,26</sup> in particular, in trauma<sup>47</sup> and surgical<sup>4</sup> patients. At the same time, different resuscitation fluids have different quantitative effects on thrombin-generation time courses.<sup>48</sup> This can be understood if we assume that the molecular components of the distinct diluents actively interact with blood coagulation proteins in distinct ways. Earlier versions of our kinetic model,<sup>7,41,43</sup> as well as its current version and results by other researchers,<sup>47</sup> predicted that dilution should considerably delay thrombin generation—an effect not observed in our own dilution experiments. This, as well as other inaccuracies in our simulations of the effects of dilution, may (at least partially) be attributed to the fact that our kinetic model does not reflect the possible effects of interactions of Na<sup>+</sup> and Cl<sup>-</sup> ions (from normal saline) with blood coagulation proteases.

The ability of hypothermia to increase ETP appears counterintuitive, but is largely consistent with our computational predictions (this work and Mitrophanov et al<sup>5</sup>) and with previous experiments.<sup>35</sup> A likely mechanistic explanation is that temperature reduction suppresses not only enzymatic conversions but also enzyme-inhibition reactions, such as the inhibition of thrombin by antithrombin, so that the net amount of thrombin is increased.<sup>35</sup> Indeed, this mechanism was represented in our computational

modeling, which predicted a hypothermia-dependent ETP increase.<sup>5</sup> At the same time, lag time in hypothermia also increased (ie, the onset of thrombin generation is delayed), which is consistent with the effects of *in vivo* hypothermia.<sup>23,25</sup> This probably occurred because the influence of the inhibitors is weaker during the initiation phase of thrombin generation. On the clinical side, the increased overall amount of thrombin produced under hypothermia could contribute to the later phases of coagulopathy in a patient, which often shifts from prohemorrhagic to prothrombotic phenotypes as coagulopathy progresses.<sup>2</sup> Alternatively, it could partially compensate for the reduced thrombin generation resulting from hypothermia-induced thrombocytopenia.

The experimentally observed effects of thrombomodulin supplementation followed somewhat unexpected patterns, which differed from our computational predictions. Under the considered conditions, the strongest thrombomodulin-dependent effects were observed in undiluted plasma, suggesting that dilution drastically reduced the activation of the protein C mechanism. It has been claimed that protein C activation—and the resultant thrombin inhibition—plays a considerable role in the onset of acute traumatic coagulopathy, which may precede significant blood dilution, hypothermia, and acidosis.<sup>49,50</sup> In that case, protein C would be activated before the dilution occurred. This scenario was not reflected in our computational model or in our *in vitro* experiments. However, the central role of the protein C mechanism in the early coagulopathy of trauma has been challenged,<sup>50,51</sup> which warrants further investigations.

Our experiments showed a very limited effect of acidosis on thrombin generation. These results complement a recent synthetic-plasma study, in which acidosis did not systematically inhibit thrombin generation.<sup>13</sup> The lack of strong thrombin-generation inhibition by acidosis *in vitro* might result from acidosis-dependent inhibition of the anticoagulant mechanisms—such as antithrombin activity—occurring simultaneously with the inhibition of the procoagulant reactions.<sup>13</sup> There were discrepancies between our experimental results and our computational modeling of the effects of pH on thrombin generation. Computational modeling of acidotic conditions in the context of trauma requires further research incorporating animal and human *in vivo* data. We surmise that *in vivo*-induced acidosis, including that in trauma and surgical patients, leads not only to alterations in pH but also to other molecular-level consequences, such as endothelial release of a stable molecular species that interferes with normal thrombin generation. This conjecture is consistent with the fact that low pH reversal cannot restore normal blood coagulation under *in vivo* acidosis.<sup>22,24</sup>

The reliance of our study on “artificial” acidification of plasma may thus be regarded as one of its limitations, and the mechanistic cause of the discrepancies between the effects of acidosis induced in vivo and those induced in vitro remains to be investigated. Another potential limitation is that we measured thrombin generation in plasma using a static assay (ie, CAT), rather than in human whole blood under flow. Moreover, the endothelium, present in vivo, can modulate the clot formation process. Further model improvements are needed for the computational simulation of thrombin generation to account for platelet activity under flow and for endothelial function. An additional source of complexity is that the effects of clinical coagulopathy may be masked by ongoing treatment and that the coagulopathic factors may be changing over time. Furthermore, the ETP can take up to 50 minutes to measure, but pathological bleeding or clotting are manifested on much shorter timescales. Thus, our results may be useful for the understanding of coagulation testing but may have limited clinical implications in the context of traumatic bleeding. Finally, our computational kinetic model did not capture some of the experimentally detected patterns and was not always quantitatively accurate. This indicates that the currently available mechanistic knowledge may not fully reflect the detailed biochemistry of thrombin generation in human plasma, as well as the dependency of thrombin generation on coagulopathic conditions. The limited number of proteins measured in individual subjects could also have contributed to the discrepancies. Nevertheless, the success in predicting a number of the experimentally observed phenomena underscores the usefulness of this approach and encourages further efforts to improve the kinetic model.

Because thrombin-generation impairment is a hallmark of coagulopathy,<sup>3</sup> understanding the effects of coagulopathic conditions on thrombin generation may facilitate the development of therapeutic strategies aimed to counterbalance coagulopathy. In vitro studies can provide preliminary assessment of such adverse effects and therapeutics, providing a foundation for subsequent animal studies and clinical investigations. A new in vivo study on the effects of prothrombin complex concentrates combined with antithrombin in a porcine model of coagulopathy suggests that computational modeling can provide insights to inform such efforts.<sup>52</sup> ■■

#### ACKNOWLEDGMENTS

The authors are grateful to Dr Tatsuya Oyama for his assistance in editing the manuscript, and to Dr Srinivas Laxminarayan, Chao Wang, and Ginu Unnikrishnan for valuable discussions regarding statistical analysis.

#### DISCLOSURES

**Name:** Alexander Y. Mitrophanov, PhD.

**Contribution:** This author designed research, performed computational modeling, analyzed data, and wrote the manuscript.

**Name:** Fania Szlam, MMSc.

**Contribution:** This author helped design the research, conducted in vitro experiments, helped analyze the data, and prepare the manuscript.

**Name:** Roman M. Sniecinski, MD.

**Contribution:** This author helped collect and analyze the data and prepare the manuscript.

**Name:** Jerrold H. Levy, MD.

**Contribution:** This author helped design the study and edit the manuscript.

**Name:** Jaques Reifman, PhD.

**Contribution:** This author designed the research, analyzed the data, and edited the manuscript.

**This manuscript was handled by:** Richard P. Dutton, MD.

#### REFERENCES

1. Cap A, Hunt BJ. The pathogenesis of traumatic coagulopathy. *Anaesthesia*. 2015;70(suppl 1):96–101, e132–e134.
2. Hess JR, Brohi K, Dutton RP, et al. The coagulopathy of trauma: a review of mechanisms. *J Trauma*. 2008;65:748–754.
3. Lier H, Krep H, Schroeder S, Stuber F. Preconditions of hemostasis in trauma: a review. The influence of acidosis, hypocalcemia, anemia, and hypothermia on functional hemostasis in trauma. *J Trauma*. 2008;65:951–960.
4. Kremers RM, Bosch YP, Bloemen S, et al. A reduction of prothrombin conversion by cardiac surgery with cardiopulmonary bypass shifts the haemostatic balance towards bleeding. *Thromb Haemost*. 2016;116:442–451.
5. Mitrophanov AY, Rosendaal FR, Reifman J. Computational analysis of the effects of reduced temperature on thrombin generation: the contributions of hypothermia to coagulopathy. *Anesth Analg*. 2013;117:565–574.
6. Mitrophanov AY, Rosendaal FR, Reifman J. Mechanistic modeling of the effects of acidosis on thrombin generation. *Anesth Analg*. 2015;121:278–288.
7. Mitrophanov AY, Szlam F, Sniecinski RM, Levy JH, Reifman J. A step toward balance: thrombin generation improvement via procoagulant factor and antithrombin supplementation. *Anesth Analg*. 2016;123:535–546.
8. Schöchl H, Grottke O, Sutor K, et al. Theoretical modeling of coagulation management with therapeutic plasma or prothrombin complex concentrate. *Anesth Analg*. 2017;125:1471–1474.
9. Tanaka KA, Mazzeffi MA, Strauss ER, Szlam F, Guzzetta NA. Computational simulation and comparison of prothrombin complex concentrate dosing schemes for warfarin reversal in cardiac surgery. *J Anesth*. 2016;30:369–376.
10. Wu TB, Wu S, Buoni M, et al. Computational model for hyperfibrinolytic onset of acute traumatic coagulopathy. *Ann Biomed Eng*. 2018;46:1173–1182.
11. Dirkmann D, Hanke AA, Görlinger K, Peters J. Hypothermia and acidosis synergistically impair coagulation in human whole blood. *Anesth Analg*. 2008;106:1627–1632.
12. Engström M, Schött U, Romner B, Reinstrup P. Acidosis impairs the coagulation: a thromboelastographic study. *J Trauma*. 2006;61:624–628.
13. Gissel M, Brummel-Ziedins KE, Butenas S, Pusateri AE, Mann KG, Orfeo T. Effects of an acidic environment on coagulation dynamics. *J Thromb Haemost*. 2016;14:2001–2010.
14. Ramaker AJ, Meyer P, van der Meer J, et al. Effects of acidosis, alkalosis, hyperthermia and hypothermia on haemostasis: results of point-of-care testing with the thromboelastography analyser. *Blood Coagul Fibrinolysis*. 2009;20:436–439.

15. Rundgren M, Engström M. A thromboelastometric evaluation of the effects of hypothermia on the coagulation system. *Anesth Analg*. 2008;107:1465–1468.
16. Whelihan MF, Kiankhooy A, Brummel-Ziedins KE. Thrombin generation and fibrin clot formation under hypothermic conditions: an in vitro evaluation of tissue factor initiated whole blood coagulation. *J Crit Care*. 2014;29:24–30.
17. Wolberg AS, Meng ZH, Monroe DM III, Hoffman M. A systematic evaluation of the effect of temperature on coagulation enzyme activity and platelet function. *J Trauma*. 2004;56:1221–1228.
18. Kheirabadi BS, Delgado AV, Dubick MA, et al. In vitro effect of activated recombinant factor VII (rFVIIa) on coagulation properties of human blood at hypothermic temperatures. *J Trauma*. 2007;63:1079–1086.
19. Darlington DN, Kheirabadi BS, Delgado AV, Scherer MR, Martini WZ, Dubick MA. Coagulation changes to systemic acidosis and bicarbonate correction in swine. *J Trauma*. 2011;71:1271–1277.
20. Darlington DN, Kheirabadi BS, Scherer MR, Martini WZ, Dubick MA. Acidosis and correction of acidosis does not affect rFVIIa function in swine. *Int J Burns Trauma*. 2012;2:145–157.
21. Dickneite G, Dörr B, Kaspereit F, Tanaka KA. Prothrombin complex concentrate versus recombinant factor VIIa for reversal of hemodilutional coagulopathy in a porcine trauma model. *J Trauma*. 2010;68:1151–1157.
22. Martini WZ. Coagulopathy by hypothermia and acidosis: mechanisms of thrombin generation and fibrinogen availability. *J Trauma*. 2009;67:202–208.
23. Martini WZ, Cortez DS, Dubick MA, Park MS, Holcomb JB. Thrombelastography is better than PT, aPTT, and activated clotting time in detecting clinically relevant clotting abnormalities after hypothermia, hemorrhagic shock and resuscitation in pigs. *J Trauma*. 2008;65:535–543.
24. Martini WZ, Dubick MA, Pusateri AE, Park MS, Ryan KL, Holcomb JB. Does bicarbonate correct coagulation function impaired by acidosis in swine? *J Trauma*. 2006;61:99–106.
25. Martini WZ, Pusateri AE, Uscilowicz JM, Delgado AV, Holcomb JB. Independent contributions of hypothermia and acidosis to coagulopathy in swine. *J Trauma*. 2005;58:1002–1009.
26. Dickneite G, Pragst I. Prothrombin complex concentrate vs fresh frozen plasma for reversal of dilutional coagulopathy in a porcine trauma model. *Br J Anaesth*. 2009;102:345–354.
27. Bladbjerg EM, Jespersen J. Activity of recombinant factor VIIa under different conditions in vitro: effect of temperature, pH, and haemodilution. *Blood Coagul Fibrinolysis*. 2008;19:369–374.
28. Gubler KD, Gentilello LM, Hassantash SA, Maier RV. The impact of hypothermia on dilutional coagulopathy. *J Trauma*. 1994;36:847–851.
29. Crawley JT, Zanardelli S, Chion CK, Lane DA. The central role of thrombin in hemostasis. *J Thromb Haemost*. 2007;5(suppl 1):95–101.
30. Hockin MF, Jones KC, Everse SJ, Mann KG. A model for the stoichiometric regulation of blood coagulation. *J Biol Chem*. 2002;277:18322–18333.
31. Butenas S, Bouchard BA, Brummel-Ziedins KE, Parhami-Seren B, Mann KG. Tissue factor activity in whole blood. *Blood*. 2005;105:2764–2770.
32. Bolliger D, Szlam F, Levy JH, Molinaro RJ, Tanaka KA. Haemodilution-induced profibrinolytic state is mitigated by fresh-frozen plasma: implications for early haemostatic intervention in massive haemorrhage. *Br J Anaesth*. 2010;104:318–325.
33. Hemker HC, Giesen P, Al Dieri R, et al. Calibrated automated thrombin generation measurement in clotting plasma. *Pathophysiol Haemost Thromb*. 2003;33:4–15.
34. Spronk HM, Dielis AW, Panova-Noeva M, et al. Monitoring thrombin generation: is addition of corn trypsin inhibitor needed? *Thromb Haemost*. 2009;101:1156–1162.
35. Dargaud Y, Wolberg AS, Luddington R, et al. Evaluation of a standardized protocol for thrombin generation measurement using the calibrated automated thrombogram: an international multicentre study. *Thromb Res*. 2012;130:929–934.
36. Semler MW, Kellum JA. Balanced crystalloid solutions. *Am J Respir Crit Care Med*. 2019;199:952–960.
37. Young R. Perioperative fluid and electrolyte management in cardiac surgery: a review. *J Extra Corpor Technol*. 2012;44:P20–P26.
38. Weiler H, Isermann BH. Thrombomodulin. *J Thromb Haemost*. 2003;1:1515–1524.
39. Brummel-Ziedins KE, Orfeo T, Rosendaal FR, et al. Empirical and theoretical phenotypic discrimination. *J Thromb Haemost*. 2009;7(suppl 1):181–186.
40. Castoldi E, Rosing J. Thrombin generation tests. *Thromb Res*. 2011;127(suppl 3):S21–S25.
41. Mitrophanov AY, Wolberg AS, Reifman J. Kinetic model facilitates analysis of fibrin generation and its modulation by clotting factors: implications for hemostasis-enhancing therapies. *Mol Biosyst*. 2014;10:2347–2357.
42. Beard DA, Qian H. *Chemical Biophysics. Quantitative Analysis of Cellular Systems*. New York, NY: Cambridge University Press; 2010.
43. Mitrophanov AY, Rosendaal FR, Reifman J. Computational analysis of intersubject variability and thrombin generation in dilutional coagulopathy. *Transfusion*. 2012;52:2475–2486.
44. Bolliger D, Szlam F, Molinaro RJ, Rahe-Meyer N, Levy JH, Tanaka KA. Finding the optimal concentration range for fibrinogen replacement after severe haemodilution: an in vitro model. *Br J Anaesth*. 2009;102:793–799.
45. Brummel-Ziedins KE, Wolberg AS. Global assays of hemostasis. *Curr Opin Hematol*. 2014;21:395–403.
46. Hemker HC, Béguin S. Thrombin generation in plasma: its assessment via the endogenous thrombin potential. *Thromb Haemost*. 1995;74:134–138.
47. Rizoli SB, Scarpelini S, Callum J, et al. Clotting factor deficiency in early trauma-associated coagulopathy. *J Trauma*. 2011;71:S427–S434.
48. Brummel-Ziedins K, Whelihan MF, Ziedins EG, Mann KG. The resuscitative fluid you choose may potentiate bleeding. *J Trauma*. 2006;61:1350–1358.
49. Brohi K, Cohen MJ, Ganter MT, Matthay MA, Mackersie RC, Pittet JF. Acute traumatic coagulopathy: initiated by hypoperfusion: modulated through the protein C pathway? *Ann Surg*. 2007;245:812–818.
50. Chang R, Cardenas JC, Wade CE, Holcomb JB. Advances in the understanding of trauma-induced coagulopathy. *Blood*. 2016;128:1043–1049.
51. Campbell JE, Meledeo MA, Cap AP. Comparative response of platelet fV and plasma fV to activated protein C and relevance to a model of acute traumatic coagulopathy. *PLoS One*. 2014;9:e99181.
52. Grottke O, Honickel M, Braunschweig T, Reichel A, Schöchl H, Rossaint R. Prothrombin complex concentrate-induced disseminated intravascular coagulation can be prevented by coadministering antithrombin in a porcine trauma model. *Anesthesiology*. 2019;131:543–554.